ASME Journal of Energy Resources Technology
Online journal at:
https://asmedigitalcollection.asme.org/energyresources

Optimal Positioning of Small Wind Turbines Into a Building Using On-Site Measurements and Computational Fluid Dynamic Simulation

Alexander Vallejo Díaz[1]
Department of Electric Engineering,
Instituto Especializado de Estudios Superiores Loyola,
Padre Ángel Arias Street, #1,
San Cristóbal, Dominican Republic
e-mail: avallejo@ipl.edu.do

Idalberto Herrera Moya
Department of Basic and Environmental Sciences,
Instituto Tecnológico de Santo Domingo,
Los Próceres Avenue #49,
Los Jardines del Norte 10602,
Santo Domingo 92000, Dominican Republic
e-mail: idalberto.herrera@intec.edu.do

Juan E. Castellanos
Department of Engineering,
Instituto Tecnológico de Santo Domingo,
Los Próceres Avenue #49,
Los Jardines del Norte 10602,
Santo Domingo 92000, Dominican Republic
e-mail: juan.castellanos@intec.edu.do

Edwin Garabitos Lara
Department of Electric Engineering,
Instituto Especializado de Estudios Superiores Loyola,
Padre Ángel Arias Street, #1,
San Cristóbal 92000, Dominican Republic
e-mail: egarabitos@ipl.edu.do

Renewable energy solutions are essential for addressing several pressing issues, including climate change, the fossil fuels supply chain fragility and fuel price fluctuations. One promising technological solution is rooftop-mounted turbines into buildings. This study presents an evaluation of the potential for wind energy utilization on the rooftop of a 29 m tall building. The primary objective of this research is to develop a methodology that can effectively investigate the integration of small wind turbines (SWTs) into urban buildings, intending to promote energy sufficiency in urban areas. A robust framework has been developed that consists of seven steps. These steps include site selection, evaluating urban wind energy with computational fluid dynamics (CFD) simulation and on-site measurements, selecting an appropriate SWT, estimating the annual energy production (AEP), conducting an evaluation of the environmental impact, resilience, and economic analysis, and finally, installing the system. This straightforward yet reliable framework provides a comprehensive approach to assessing the viability of wind energy utilization in urban areas. The findings revealed that the most suitable location for installation had an estimated AEP of around 1030 kWh, leading to a reduction in emissions of 0.64 tCO_2/y. Additionally, it was observed that the building's geometry and orientation significantly affected the wind flow, causing a substantial decrease in wind speed downstream. Selecting optimal sites and considering wind patterns are essential for maximizing energy generation in wind energy projects.
[DOI: 10.1115/1.4065381]

Keywords: urban wind energy assessment, distributed power system, small wind turbine, CFD, Dominican Republic

1 Introduction

Controlling the escalating risks posed by climate change requires an immediate decarbonization of the global energy sector. Global average temperature for August 2022 was 0.3 °C higher than from 1991 to 2020 [1]. However, there exist other risks associated with an economy reliant on fossil fuels. The finite supply of fossil fuels, the concentration of these resources in a small number of countries, and the volatility of the energy market are crucial factors that weigh the pros and cons of the various sources. The United States, Saudi Arabia, and Russia led the top three oil producers, with 21%, 13%, and 10%, respectively, and the top ten accounts 74% globally [2].

Energy transition is imperative to tackle climate change. This shift needs to be addressed in the energy trilemma of energy security, energy equity, and environmental sustainability. The industry must navigate these complex issues and find solutions that effectively balance all three dimensions [3]. On the other hand, the rise in fuel prices (especially natural gas) in Europe is an obvious illustration of how the fuel market can shift in a relatively short period of time with grave implications for national economies due to external factors such as the pandemic, war, and geopolitical issues [4]. For example, the Dutch TTF natural gas increased from 79 to 210 EUR/MWh in roughly three months [5]. More than ever, governments, scientists, and politicians recognize the urgency of advancing alternative energies. To expedite the energy transition towards carbon-free services and to gradually deploy renewable energies, wind and solar photovoltaics (PV) are essential building blocks. The growth rates of wind and PV power were considerably high in 2021, increasing by 14% and 23%, respectively. Wind and solar power must continue to grow at high compound growth rates of 20% annually through 2030, the same rate as the

[1]Corresponding author.

Contributed by the Advanced Energy Systems Division of ASME for publication in the Journal of Energy Resources Technology. Manuscript received December 13, 2023; final manuscript received March 25, 2024; published online May 24, 2024. Assoc. Editor: Tatiana Morozyuk.

previous ten years, in order to keep global warming on track at 1.5 °C [6].

Building consumption represents approximately 30% of primary energy consumption globally [7]. In the United States building consumption accounts 40% of total energy, making it crucial to achieve carbon neutrality through energy efficiency and the use of renewable energy sources [8]. Energy efficiency can result in savings of 20%–40%. According to Millward-Hopkins et al. [9], small wind turbine (SWTs) installations are anticipated to support the shift to low-carbon energy and improve urban energy efficiency. Urban areas have high population densities, drawing attention to the need for specific energy solutions, particularly close to the demand area, decentralized generation, such as PV and SWTs systems [10].

The utilization of urban wind energy could make a significant contribution to the expansion of wind power. The lack of available land in urban areas, however, is thought to be a significant barrier to the installation of large machines. Integrating wind energy systems into urban areas is an alternative. The ability to use produced energy on-site, thereby avoiding transportation losses and producing extra economic benefits, is a major benefit of this distributed renewable technology. There is enough wind to produce considerable microgeneration from this energy source when set up properly, especially in the vicinity of tall buildings. A systematic analysis is required to guarantee the feasibility of projects in urban wind energy harnessing [11].

Innovative energy solutions are necessary to produce clean, safe, and environmentally friendly energy to tackle the energy deficit, environmental pollution, and other issues pertaining to sustainable development. Wind energy, both large- and small-scale, is an alternative that is expanding quickly worldwide [12]. In extremely densely populated urban areas, there is great potential for distributed electricity generation using urban wind [13]. SWTs offer great potential for use in domestic installations, on building roofs or in surrounding areas, or even integrated into buildings from the design stage [14]. Reduction in the cost of high voltage transmission lines and control devices is another benefit of using wind energy in cities due to its close proximity to demand [15].

According to Rezaeiha et al. [16], wind energy systems can be classified into three groups, such as turbines installed in close proximity to buildings, retrofitted in existing building, or buildings that have turbines integrated into their architectural design. SWTs can be positioned in high-rise buildings, railroads, roadways, and other urban locations [17]. Since the cities are heterogeneous places and aerodynamically irregular, estimating wind energy becomes extremely difficult. Obstacles such as trees, buildings, and other objects produce turbulence in the wind flow [12]. The obstacles extract momentum from the wind flow and significantly reduce energy capture by the SWTs [18].

Toja-Silva et al. [15] used computational fluid dynamics (CFD) simulations to present an analysis of multidirectional wind conditions. The authors examined a SWT located on a building's roof and its different behaviors. According to the flow fields, horizontal axis wind turbines (HAWTs) need to be positioned higher above the building's roof, whereas vertical axis wind turbines (VAWTs) perform better in turbulent impalements. To make the computational process easier for users with limited numerical method experience, Gagliano et al. [19] assessed the potential of wind energy in Italy using CFD simulation within a geographic information system (GIS). The best locations for the installation of SWTs in urban settings can be found using this methodology. According to Dhunny et al. [20], wind flow in complex terrain can be evaluated using CFD and validated using on-site measurements. The WindSim tool was utilized to create the wind map of Mauritius, and nine anemometric stations located across the island confirmed the accuracy of the map. The turbulence model, the discretization strategy, and the convergence criterion are emphasized in this study. Based on a thorough bibliometric review, Toparlar et al. [21] demonstrated the exponential trend in the use of this tool in publications pertaining to microclimate over the previous 20 years. Moreover, the tropical region lacked studies using CFD simulation. It is noteworthy that there are very few CFD studies conducted in Latin American countries, particularly in the Caribbean region. Significant conclusions about where to place SWTs on building roofs have been reached through CFD simulation. In 2018, Stathopoulos et al. [22] suggested placing HAWTs 1.4 m above building roofs and in the center of the roof. HAWT placement thresholds are 30% of the building height, while vertical axis wind turbine (VAWT) placement thresholds can be lower [23].

Arteaga-López et al. [24] provided a methodology for characterizing the urban wind potential in a Mexican university building, primarily considering the SWT's characteristics and the building's morphology. A 10 kW Bergey Excel SWT can generate enough energy for the campus' self-consumption or to light the public areas. The best configuration determined by the CFD simulations showed that the building under consideration can only accommodate five SWTs which are suitable to the building's annual energy demand. The CFD results were validated with the experimental results. Juan et al. [25] used CFD simulation to assess the effects of urban morphology on the utilization of urban wind energy for high-rise building arrangements. They adopted three-dimensional Reynolds-averaged Navier–Stokes (RANS) stable equations and verified their findings with wind tunnel measurements. The findings showed that turbulence and the beneficial effect of rounded corners increase with urban area density. To comprehend the relationship between the wind inside and outside the urban canopy layer (UCL). Ricci et al. [26] created a methodology for estimating urban wind within the UCL using on-site measurement and CFD simulation. They also pointed out the drawbacks of 3D Steady RANS simulations in two case studies. Table 1 lists the Scopus top publications which frameworks include CFD simulation in the resource assessment stage.

Computational fluid dynamics simulations can be effectively integrated into urban wind energy assessment techniques. In principle, these studies aim to characterize air flow through obstacles such as buildings and trees in a controlled volume. In an urban environment, the flow is considered turbulent. Earlier studies on building-mounted wind turbine installation in urban environments applying CFD analysis have shown results that indicate that SolidWorks Flow Simulation software is appropriate for this task [24].

Urban wind energy assessment is a complicated process due to the high turbulence and complex orography of cities. Since the project's viability is heavily dependent on the estimate of energy produced, a thorough evaluation of the resource is essential. Numerous approaches have been proposed, such as site selection, wind

Table 1 Urban wind energy potential analysis studies through CFD

No.	References	Authors (year)	Countries
1	[15]	Toja-Silva et al. (2013)	Spain
2	[27]	Padmanabhan (2013)	India
3	[19]	Gagliano et al. (2013)	Italy
4	[28]	Park et al. (2015)	South Korea
5	[14]	Simões and Estanqueiro (2016)	Portugal
6	[29]	Toja-Silva et al. (2016)	Japan
7	[13]	Yang et al. (2016)	Taiwan
8	[30]	Khoshdel Nikkho et al. (2017)	United States
9	[12]	Wang et al. (2018)	China
10	[24]	Arteaga-López et al. (2019)	Mexico
11	[31]	Wang et al. (2020)	South Korea
12	[32]	Vita et al. (2020)	United Kingdom
13	[33]	Arteaga-López and Angeles-Camacho (2021)	Mexico
14	[34]	Juan et al. (2021)	China
15	[25]	Juan et al. (2021)	China
16	[35]	Mitkov et al. (2022)	Bulgaria
17	[26]	Ricci et al. (2022)	Italy

speed estimation, small wind turbine selection, annual energy production estimation, economic assessment, and environmental analysis [36,37]. The framework presented by Rezaeiha et al. [16], is interesting since it makes use of software that is freely accessible for calculating the quantity of suitable building's rooftops in The Netherlands according to their height. A methodology that included financial profitability and avoidance of greenhouse gas emissions was recently presented [37]. This methodology complemented the previous one. Conversely, to supplement current methodologies, [38] has suggested including an analysis of energy resilience. The vulnerability that has widely dispersed SWTs in cities vulnerable to atmospheric events (hurricanes and tropical storms) in tropical zones, forms the basis of the authors' contribution. The availability and dependability of SWT systems integrated into buildings during the project's life (CAPEX and OPEX), which is typically 20 years, are also impacted by other low-probability and high-impact events, which must be considered. Moreover, Vallejo-Díaz et al. [39] have presented a hybrid Strengths, Weaknesses, Opportunities, and Threats–Analytic Hierarchy Process (SWOT–AHP) analysis that combines qualitative and quantitative approach. The authors also presented a complementary analysis to bring a wider perspective in decisions making. The goal of the authors' analysis was to pinpoint the major variables that have shaped technology development thus far. Thus, non-technical analyses that support the growth and application of urban wind energy can be conducted. Another tool used to identify stakeholders and their roles in projects or management is Responsible, Accountable, Consult, and Informed (RACI) [40]. The RACI matrix can be applied to the energy sector to identify the responsible actors [41]. It is important to complement the methodologies with organizational tools for decision making, since these shed light on hidden factors. In every technology deployment, decision-makers must converge with clear and precise roles and assignments [42]. Recently, Vallejo-Díaz et al. [43] presented a RACI analysis applied to the stakeholders at the national level that influence urban wind energy in the Dominican Republic. A total of 59 interviews were carried out, and 28 public and private institutions were evaluated. According to the experts' judgment, the prominent institutions were the Ministry of Energy and Mines (A), electricity distribution companies (R), energy associations and universities (C), and educational and justice institutions (I).

This work's primary contribution is the technique it suggests, which combines several different approaches to provide a comprehensive analysis of the research on urban wind energy. The technique considers a seven-step framework that is thorough. In the resource analysis step, the impact of location on energy production is studied using CFD modeling and in situ measurements. The purpose of this research is to help determine the best location for SWTs on building roofs. A case study in the Dominican Republic, which has a tropical climate, uses the methodology to determine the best positioning of a SWT to maximize the power produced by urban wind kinetic energy, using on-site measurements and several CFD simulations. The structure of this research is as follows: Sec. 2 describes the proposed methodology approach. Section 3 outlines the case study. In Sec. 4, results and discussion are presented. Finally, in Sec. 5, the conclusions are given.

2 Materials and Methods

The proposed methodology adopts several steps from some existing ones that have been published separately. This framework proposes to consolidate all the contributions of existing methodologies to achieve an integrated analysis of urban wind energy study. The proposed methodology is presented in three phases in Fig. 1. The first phase is about the evaluation of urban wind energy. This contains the seven steps such as (1) site selection, (2) wind resource analysis including using on-site measurements and CFD simulation, (3) small wind turbine selection, (4) annual energy production estimation, (5) environmental evaluation, (6) resilience and economic analysis, and (7) system installation. The second phase is concerned with identifying the key factors and prioritizing them. This phase is composed of two main steps, which are the determination of the key factors through a SWOT analysis and the prioritization of these factors through paired comparison with the AHP analysis [44]. Finally, the third phase proposes integrating the RACI matrix into the methodology to identify key stakeholders in the urban wind energy sector in three steps such as interviews with experts, role diagnoses, and stakeholder mapping in the RACI Matrix. This research focuses on the first phase, especially on the wind energy assessment. The second and third phases have been well described in previously cited investigations [39,43].

2.1 Site Selection and Characterization. The choice of urban location for incorporating the SWTs is critical. Wind speeds in cities are typically low due to the obstacles in the urban morphology [36].

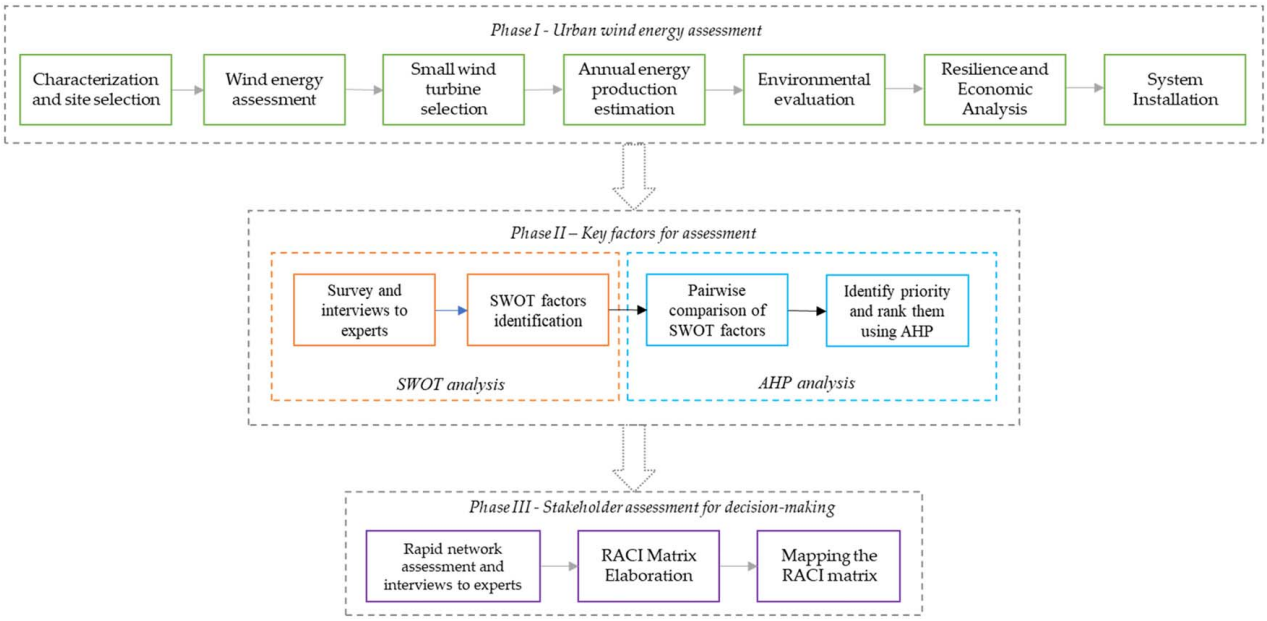

Fig. 1 The proposed methodology illustrated by phases and steps

However, there is a lot of space available above buildings in cities that can be used for harnessing wind energy [45]. GIS tools can be used to identify these areas [46] or even in the data provided by the local urban planning authority. According to Vallejo et al. [45], Santo Domingo has great potential in tall buildings, especially those 90 m high, because the wind flows faster, and thus, more energy is produced, ensuring that the levelized cost of energy is comparable to the cost of the distribution network. Therefore, taller buildings are the most attractive to install SWTs since the wind flows faster at higher altitudes.

2.2 Wind Energy Assessment. Several methods for prospecting and studying urban wind have been reported in the literature. On-site measurement, CFD simulation, numerical climate prediction (NWP), wind tunnels, and analytical methods are the most common [11,29,47]. These methods take different approaches from morphological and meteorological scales [48]. Typically, the NWP is used to examine the region in a mesoscale spatial resolution, on-site measurement is focused on local resolution or neighborhood scales, and finally the CFD simulation to microscale and consider the building details. The NWP may overestimate the potential because it does not account for terrain roughness and other aspects of thermal conductivity [38,49]. The main goal is to determine the wind speed, direction, turbulence, and energy density in the studied area.

On the other hand, the wind tunnel can be useful in determining a wide range of variables that cannot be determined using CFD simulation [22,50], but this is beyond the scope of this study. Analytical methods, which can be used to predict wind speed in urban areas [51], are less common in the reported literature [38]. This study utilizes on-site measurements and CFD simulation to identify the optimal location for SWT on a building's rooftop. Each method is described in more detail below.

2.2.1 On-Site Measurement. This is the most popular approach to wind energy assessment because it provides precise information about the wind in each location. In order to measure wind speed and direction as well as other meteorological variables, this method entails installing sensors (vanes, pyranometers, pyrometers, and anemometers), datalogger and other devices at the site of interest [38]. When assessing the potential for wind energy generation in urban areas, on-site measurement is particularly helpful because buildings and other obstacles, as well as the local topography, can affect wind variability. It is crucial to choose the measurement station's position to guarantee the collection of precise and representative datasets. In addition, the period of measurement campaigns and the data analysis are crucial for assessing the wind variability and wind energy generation potential at the site of interest [52]. The Weibull, Rayleigh, and Lognormal distributions are used to determine the most probable wind speed during a year. Weibull distribution is the most used due to its simplicity and adaptability [53]. The Weibull probability density function $p(V_{\text{avg}})$ is shown in Eq. (1), where c is the scale factor in m/s and k is the shape factor. The average wind speed (V_{avg}) and the shape of the distribution, which are defined in Eq. (2), are controlled by the parameters k and c, respectively.

$$p(V_{\text{avg}}) = \left(\frac{k}{c}\right) * \left(\frac{V_{\text{avg}}}{c}\right)^{k-1} e^{-\left(\frac{V_{\text{avg}}}{c}\right)^{k}} \tag{1}$$

$$c = \frac{V_{\text{avg}}}{\sqrt{\pi}} \tag{2}$$

The wind speed used for a probability estimate must be measured at the hub height and this can be estimated with Eq. (3), also known as the Hellmann's power law [54], where V_i is the desired velocity at height Z_i, V_0 is the known velocity at height Z_0, and α is the Hellmann exponent [55].

$$V_i = V_0 * \left(\frac{Z_i}{Z_0}\right)^{\alpha} \tag{3}$$

2.2.2 Computational Fluid Dynamics. CFD is a widely used scientific approach for studying wind flow patterns in urban areas [56]. By integrating the Navier–Stokes equations at the turbine blade periphery, CFD models can accurately predict aerodynamic components [57]. CFD offers an efficient alternative for characterizing wind turbulence around buildings. Over time, CFD methods have undergone significant improvements in terms of simplification, calculation models, mesh processing, boundary conditions, equation solvers, simulation tools, and other aspects [12]. SolidWorks Flow Simulation employs the RANS equations and turbulence models to simulate turbulent flows, shown in Eqs. (4) and (5). The RANS equations, which are the time-averaged form of the Navier–Stokes equations, are solved to describe the conservation of mass, momentum, and energy for fluid flow and assume that the flow variables can be decomposed into mean and fluctuating components. The most used turbulence model is the standard k-epsilon ($k-\varepsilon$) model, as shows in Eq. (6). It assumes that the turbulent viscosity is proportional to the turbulent kinetic energy and the turbulent length scale. The $k-\varepsilon$ model solves transport equations for the turbulent kinetic energy and its energy dissipation rate, which are then used to compute the turbulent viscosity and incorporate its effects in the RANS equations [58,59]. While more sophisticated turbulence models could be used, the k-epsilon model provides adequate accuracy for the current task [24], as shown in Eqs. (4), (5), and (6), well presented in Ref. [59].

$$\frac{\partial \rho k}{\partial t} + \frac{\partial \rho k u}{\partial x_i} = \frac{\partial}{\partial x_i}\left(\left(\mu + \frac{\mu_k}{\sigma_k}\right)\frac{\partial k}{\partial x_i}\right) + \tau_{ij}^{R}\frac{\partial u_i}{\partial x_j} - \rho\varepsilon + \mu_t P_B \tag{4}$$

$$\frac{\partial \rho \varepsilon}{\partial t} + \frac{\partial \rho \varepsilon u_i}{\partial x_i} = \frac{\partial}{\partial x_i}\left(\left(\mu + \frac{\mu_k}{\sigma_\varepsilon}\right)\frac{\partial \varepsilon}{\partial x_i}\right) + C_{\varepsilon 1}\frac{\varepsilon}{k}\left(f_1 \varphi_{ij}^{R}\frac{\partial u_i}{\partial x_j} + C_B \mu_t P_B\right) - f_2 C_{\varepsilon 2}\frac{\rho\varepsilon^2}{k} \tag{5}$$

$$\tau_{ij} = \mu S_{ij},\ \ \tau_{ij}^{R} = \mu_t S_{ij} - \frac{2}{3}\rho k \delta_{ij},\ s_{ij} = \frac{\partial \mu_i}{\partial x_j} + \frac{\partial u_j}{\partial x_i} - \frac{2}{3}\delta_{ij}\frac{\partial u_k}{\partial x_k} \tag{6}$$

$$P_B = -\frac{g_i}{\sigma_B \rho}\frac{1}{\partial x_i}\frac{\partial \rho}{\partial x_i} \tag{7}$$

where $C_\mu = 0.09$, $C_{\varepsilon 1} = 1.44$, $C_{\varepsilon 2} = 1.92$, $\sigma_k = 1$, $\sigma_\varepsilon = 1.3$, $\sigma_B = 0.9$, $C_B = 1$ if $P_B > 0$, $C_B = 0$ if $P_B < 0$ the turbulent viscosity is determined from Eq. (8).

$$\mu_t = f_\mu * \frac{C_\mu \rho k^2}{\varepsilon} \tag{8}$$

Lam and Bremhorst's damping function f_μ are determined from Eqs. (9), (10), and (11), where y is the distance from point to the wall and Lam Bremhorst's damping functions f_1 and f_2 are determined from Eq. (12). Lam and Bremhost's damping functions f_μ, f_1, f_2 decrease turbulent viscosity and turbulence energy and increase the turbulence dissipation rate when the Reynolds number R_y based on the average velocity of fluctuations and distance from the wall is too small. When $f_\mu = 1$, $f_1 = 1$, and $f_2 = 1$, the approach reverts to the original ($k-\varepsilon$) model.

$$f_\mu = (1 - e^{-0.025R_y})^2 * \left(1 + \frac{20.5}{R_t}\right) \tag{9}$$

$$R_y = \frac{\rho\sqrt{ky}}{\mu} \tag{10}$$

$$R_t = \frac{\rho k^2}{\mu \varepsilon} \tag{11}$$

$$f_1 = 1 + \left(\frac{0.05}{f_\mu}\right),\ f_2 = 1 - e^{R_t^2} \tag{12}$$

However, the accuracy of CFD results, associated costs, and user expertise remain the primary barriers to its popularity. Consequently, verification and evaluation of CFD simulation results are crucial. Typically, validation for CFD studies in real urban settings is conducted using field measurements and wind tunnel experiments [47,56,57].

Mittal et al. [47] emphasize that the accuracy of CFD simulations heavily relies on the choice of turbulence model. Researchers have reported on the capabilities and precision of different turbulence models for various analysis resolutions. Notably, significant insights have been gained through this approach, such as the recommendation to install SWTs approximately 1.4 m above building roofs. Furthermore, for HAWTs, it is recommended to place them in the middle of the roof and as high as possible in the windward direction [22]. In urban areas, wind speeds are generally lower compared to rural open areas. Consequently, it is essential to leverage points within buildings where flow accelerates to achieve a substantial increase in power density, potentially reaching three–eight times higher than the average power density [60].

In order to assess the feasibility of the project, it is crucial to define the project location and its surrounding area, as mentioned in Sec. 2.1. Utilizing CFD simulations, a comprehensive understanding of wind flow patterns within the urban complex can be achieved. This aids in predicting the behavior of wind streams and evaluating the performance of SWTs installed on the roofs of specific buildings. After selecting the site, a standard wind resource assessment is conducted to estimate the power output of SWTs. This assessment utilizes statistical datasets. The next step involves a (CFD)-based assessment, which consists of four stages: site assessment modeling, building-structure modeling, SWT modeling, and structure-SWT modeling. These stages involve creating a CFD model of the site, including the building and its surroundings, as well as a model of the building or structure specifically designed for CFD analysis. This analysis aids in determining the most suitable type of turbine to be installed.

After the SWTs are selected, a performance study utilizing CFD analysis should be carried out. The results of this comprehensive analysis, using SolidWorks Flow Simulation and applying finite volume analysis [61], will determine the technical viability of the project.

2.3 Selection of Small Wind Turbines. SWTs are emerging urban power generation technologies that are gradually being integrated into buildings, and peripheral environments and are even considered in civil structure architectural design [19,22]. Building-integrated wind turbine systems are classified as large or small, with small ones being more convenient and cost-effective in terms of building structural modification [28]. SWTs are machines that have the ability to extract kinetic energy from the wind flow and convert it into electricity via the aerodynamic forces induced on the blades [62]. Electricity generation is proportional to the cube of wind speed, swept area of turbine blades, and air density [63]. Figure 2 shows the primary SWTs designs, which are primarily HAWTs and VAWTs. The VAWTs are classified as Savonius, Darrieus, and H-rotor type [22,64]. Darrieus and Savonius work by the action of the lift force and the drag force, respectively. VAWTs are the most used in urban areas because they are omnidirectional, operate at a lower speed, and account for better three-dimensional aesthetics that can make them more popular whereas HAWTs must always be oriented with the rotor

Fig. 2 Taxonomy of (*a*) vertical axis turbines and (*b*) horizontal axis turbines, Ref. [22]

perpendicular to the wind direction, they are ideal for mountainous places that have a constant gust of wind [65,66]. Darrieusis more suitable for low- to medium-wind speed areas; however, the cross-sectional profile of blades is a key parameter to keep the efficiency in the design stage [67]. HAWTs are less commonly encountered in the literature. These machines are installed in larger areas with significant heights above ground level, in accordance with local policies and regulations. The most appropriate type is determined by wind speed, installation and operation flexibility, height limitation, and aesthetic integration into the urban built environment [56].

According to the International Electrotechnical Commission (IEC) standard [68], SWTs must have a capacity of 50 kW and a rotor-swept area up to 200 m^2. China, Germany, UK and United States have different classifications based on power, hub height, and swept area [16]. On the other hand, SWTs are classified into four categories based on rated power: micro (less than 10 kW), mini (10–100 kW), median (100–1000 kW) and large (greater than 1000 kW) [69].

Because VAWTs are less sensitive to changes in wind direction, they have a lower manufacturing cost because they lack a yaw mechanism, and as a result, fewer failures occur [70]. The HAWT and Darrieus are lift SWTs, and the Savonius is a drag SWT [71]. Tan et al. [72], presented a review of Savonius-Darrieus hybrid radial, counter-rotating and rotor wind turbines, particularly for low wind speed operation and noise reduction. They demonstrated that redesigning the chimney's height and the volute-shaped structure triples the power coefficient. They also discussed the benefits of piezoelectric generators and triboelectric nanogenerators for SWTs. Lipian et al. [73], on the other hand, presented an analysis using CFD simulation for the optimization of multi-rotor revolver-type SWTs, demonstrating that the relationship between the angle of attack and the velocity fields in the plane of rotation is relatively robust. Fatigue load characteristics, dynamics loads, and Taguchi Technique have been evaluated to the adequate laminate stacking sequence and lamina angles for the composite blade of Savonius VAWT [74].

Turbine positioning is critical because turbine performance can be hampered by low wind speed, high turbulence, or high noise levels produced by the turbine [71]. Several analyses using CFD simulation have been performed to study the optimal positioning of SWTs on building roofs of various shapes. Turbulence in the flow has been measured to extend up to 1.3 times the height of the building [75]. The authors believe that determining the optimal positioning of the SWTs in tropical environments while considering the morphology of the countries involved would lead to very interesting future research. To demonstrate that the turbines meet the levels of performance, durability, and other quality aspects and metrics used for comparison, SWTs must be certified by a competent standard. Some critical aspects include safety, acoustic level requirements, structural resistance, and so on. A list of certified SWTs and the best practices are presented by the American Wind Energy Association (AWEA) [76].

2.4 Annual Energy Production Estimation. Combining the SWT power curve and the characteristics of the wind flow, the Annual Energy Production (AEP) is determined prospectively for a certain period [77]. The available energy can be determined approximately with Eq. (13), where C_p is the power coefficient, ρ is the air density, A is the swept area, and V_{avg} is the average wind speed [55].

$$P_V = \frac{1}{2} C_p \rho A V_{avg}^3 \tag{13}$$

The AEP estimate considerably influences the levelized cost of electricity (LCOE) from the distributed generation system. As the AEP increases, the LCOE decreases, according to the sensitivity analyzes presented by Olatayo et al. [78]. With Eq. (14), the AEP can be determined for a year, where we have a combination of Eqs. (1) and (13) [39].

$$\text{AEP} = 8760 \times \int_0^\infty P(V_{avg};\, c;\, k) P(V_{avg})_{dv} \tag{14}$$

2.5 Environmental Evaluation. As the world's population grows, more environmentally friendly energy sources are needed to mitigate the negative effects of air pollution. In this sense, the world is in the process of decoupling economic growth from reliance on fossil fuels. Small-scale distributed power generation solutions have a high potential to reduce environmental impact, though the effects are not immediate [79]. To assess the potential environmental benefit of installing SWTs, the mitigation result in terms of reduced greenhouse gas emissions is assessed [80]. The annual avoided emissions can be calculated by multiplying the amount of energy consumed (replaced from the grid) by the emission factor of the respective electrical grid [81], as shown in Eq. (15).

$$\text{AES} = \text{AEP} \times \text{FE} \tag{15}$$

where AES is the annual emissions savings in tCO_2e per year, AEP is the annual energy produced in the system in MWh, and FE is the grid emission factor in tCO_2e/MWh for an electricity system according to the Clean development Mechanism, well presented by the United Nations Framework Convention on Climate Change [82].

2.6 Resilience and Economic Analysis. Naturally occurring catastrophes and other high-impact low-probability (HILP) occurrences put power systems at risk of both operational and infrastructural harm. To adopt adaptive measures in the face of such occurrences, resilience metrics are therefore required to measure the effect and vulnerability [83]. Reliability is the lens through which events with low-impact high-probability (LIHP) are examined. Relational dependability to HILP and resistance to LIHP are the most widely held presumptions [84]. According to Selga et al. [84], distributed renewable energies, such as SWTs integrated into buildings, can be a solution to prevent and mitigate the vulnerability and cascading failure of distribution networks when they are affected by climatological threats. The authors classified the threats into three groups, such as, catastrophic weather events, cyber-attacks, and sudden changes in the use of network infrastructure (the effect of the COVID-19 pandemic). As meteorological threats due to climate change increase, the intensity of these events significantly reduces the resilience indices of distributed energy systems such as urban wind energy. Engineers and academics must formulate proposals that improve the resilience of the system proportionally based on the potential threat to each of the generation technologies to achieve independence of energy systems and achieve their alternation [85].

Vallejo-Díaz et al. [38] proposed a preliminary approach to incorporate the economic implications of atmospheric events into the analysis of SWTs projects. This is crucial considering the Dominican Republic's susceptibility to such events, with 17 atmospheric occurrences affecting the country in the past two decades. Three scenarios were determined to evaluate the resilience of urban wind energy. In the first scenario, the SWTs system resists the predicted atmospheric event due to its wind speeds are below the operational threshold. This scenario applies to tropical storms or Category 1 hurricanes. In the second scenario, the SWTs system is disassembled in order to anticipate the disaster of the system due to the forecasted atmospheric events surpassing the wind turbines' functional limit. Consequently, there are costs associated with disassembly and reassembly. Finally, in the third scenario, the SWT system's functioning is harmed since it was not disassembled in the case of an atmospheric event. In this instance, restoring the SWTs system will cost more money. Over the last 50 years, tropical cyclones have caused approximately 2000 disasters, resulting in human deaths and economic losses, with an average of 43 deaths and US$78 million in damages per day [86].

The cost of wind power electricity is an important factor to consider, especially in small-scale systems that require proper evaluation for financing [87]. The total costs associated with the concentrated energy market include generation costs (power, capacity, and ancillary services), transmission and distribution costs, and marketing costs, as well as government subsidies in cases where end users do not receive price signals [88]. The authors presented a detailed comparison of different approaches to calculating the LCOE, outlining each method's strengths and weaknesses. The one that discounts energy and cash flow amounts over the course of the project is the most widely used. In addition, each country must consider other fiscal and economic incentives.

2.7 System Installation. This final stage has to do with the implementation of the project. It is an engineering job. In this case, it is recommended to follow NREL's best practices, well presented by Fields et al. [18].

3 Case Study

A case study was carried out at the Santo Domingo Institute of Technology (INTEC), to determine the potential of urban wind energy and the best SWT positioning on the building rooftop. INTEC is located at 18 deg29′16.81″N, 69 deg57′45.18″W. During 2017, two anemometers (Anem1-INTEC and Anem2-INTEC) were collecting data. The Anem1-INTEC recorded data from May to December in 2017, and Anem2-INTEC from June to December in the same year. Both anemometers were installed in a building 22.5 m height above the ground. A total of 208,881 and 152,816 records were taken from Anem1-INTEC and Anem2-INTEC, with an availability of 71% and 77%, respectively. Figure 3(*a*) shows the physical model of the INTEC campus and Fig. 3(*b*) the Eduardo Latorre (EL) building and sites of interest (EL building).

This study evaluates the INTEC campus with numerical simulation to determine the best positioning of the turbines in the geometry of the building's roof. The main idea is to determine the optimal positioning from the data records obtained in a field measurement campaign, which contains the wind flow pattern at the site of interest.

4 Results and Discussion

The findings from the case study conducted on the INTEC campus are presented in this section, with a focus on the assessment of urban wind energy for the production of electricity. Figure 4(*a*) shows the monthly average wind speed of Anem2-INTEC. The average wind speed at a height of 22.5 m was approximately 2.49 m/s during the periods under consideration. However, at a height of 34 m, the estimated average wind speed, using the Hellmann exponential law, wind profile law, was found to be 3.05 m/s. This approach allows for the extrapolation of wind data to higher elevations, providing valuable insights into wind patterns and velocities at different heights. A wind rose diagram is shown in Fig. 4(*b*), where the prevailing direction is 15 deg to the north, indicating that the wind is most frequently coming from the north-east.

Figure 5(*a*) depicts the intensity of wind speed over the course of a 24-h period. Records were used to construct the Weibull probability density function in accordance with the IEC standard; the probability density function is shown in Fig. 5(*b*). The Weibull distribution parameters for a wind speed of 3.05 m/s were determined to be 3.44 m/s and 2.00 for the shape factor and scale factor, respectively. Additionally, the turbulence intensity was measured to be 63%, 29%, and 8%, indicating moderate, high, or low levels, respectively. These findings can be attributed to the terrain

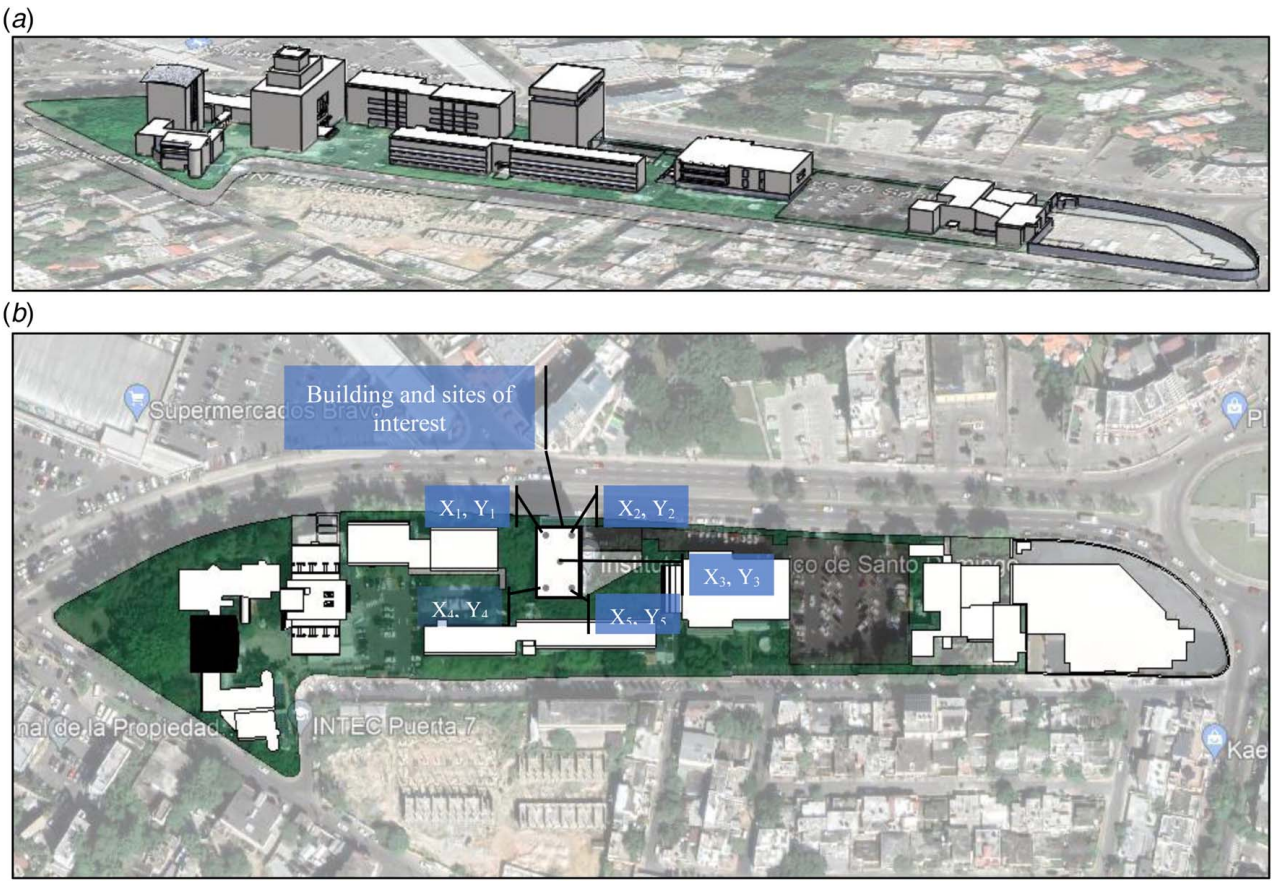

Fig. 3 (*a*) Physical model of the INTEC campus and (*b*) building and sites of interest (EL building)

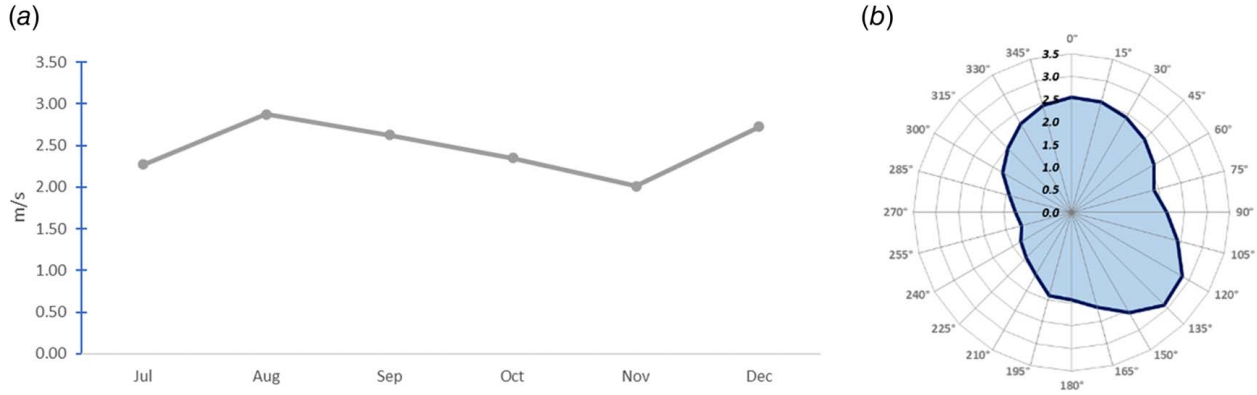

Fig. 4 (*a*) Average monthly wind speed and (*b*) period average wind rose

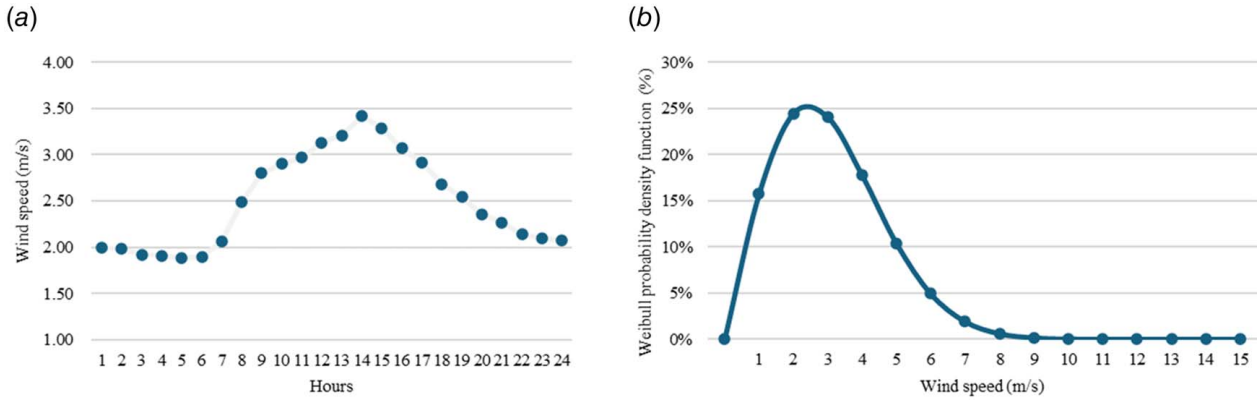

Fig. 5 (*a*) Daily variation of wind speed and (*b*) Weibull probability density function

Table 2 Boundary conditions for the development of CFD simulations

Analysis type	Fluid type	Boundary conditions	Initial and environment conditions	Mesh configuration
Flow Type: External Gravity force: 9.81 m/s^2	Air with all its physical properties Laminar and turbulent flow	Roughness length: 1,000,000 μm	(a) Thermodynamic parameters: – Temperature 28 °C = 301 K – Atmospheric pressure: 101,325 Pa (b) Velocity parameters: (c) speed of air 1 m/s, 2 m/s, 3 m/s, 4 m/s, 5 m/s, 6 m/s 7 m/s, 8 m/s, at 15 deg (d) Turbulence parameters: – Turbulence length: 0.4003 m – Turbulence intensity: 0.1% (e) Humidity parameters: – Average relative humidity of 80%	Manual mesh with 2,643,484 control volume cells

orography as the measurements were taken in an urban environment. The presence of buildings and other structures in urban areas can cause variations in wind patterns, resulting in different turbulence intensities. Understanding these factors is crucial for accurately assessing wind conditions and optimizing the urban wind energy generation.

Table 2 provides a detailed description of the initial conditions chosen for the CFD simulations conducted in this study. The wall condition of 1,000,000 μm was determined based on the "Guide to Meteorological Instruments and Methods of Observation," which classifies terrain roughness based on terrain class [89]. The INTEC campus is surrounded by class 7 terrain, characterized by large regular obstacles commonly found in suburban areas, resulting in a roughness height of 1 m.

The configuration of the grid and the refinement of the mesh play a crucial role in ensuring the precision of the CFD simulations. In this study, global mesh structures were selected, with a manual refinement definition of 249 cells per X, 100 cells per Y, and 100 cells per Z. Global mesh refinement surpasses the number of cells assigned in all axes through the highest level of auto refinement, aiming to guarantee precision in the areas of interest. This results in a total of 2,643,484 cells in the mesh, with 78,416 cells in contact with solids. In addition to mesh refinement, a control

Table 3 Summary of the mesh size test

Mesh size cells per axis			Freestream parameters		Measured data	CFD Results		WS Error (%)
X	Y	Z	WS (m/s)	WD (deg)	WS (m/s)	WS (m/s)	WD (deg)	
123	49	50	2.99	62.30	2.44	3.15	55.94	22.4
249	100	100	2.99	62.30	2.44	2.23	55.65	9.4
500	200	100	2.99	62.30	2.44	2.22	57.67	9.8

Table 4 Comparison between measured datasets versus simulated results

Date				Freestream parameters		Measured data	Modeling results		Relative error	
Year	Month	Day	h	WS (m/s)	WD (deg)	WS (m/s)	WS (m/s)	WD (deg)	WS (%)	WD (%)
2017	8	12	22	1.80	129.9	1.45	1.46	127.3	0.6	2.0
		21	4	2.96	72.6	2.49	2.50	67.1	0.6	8.1
		27	3	2.99	62.3	2.44	2.23	56.2	9.4	10.8

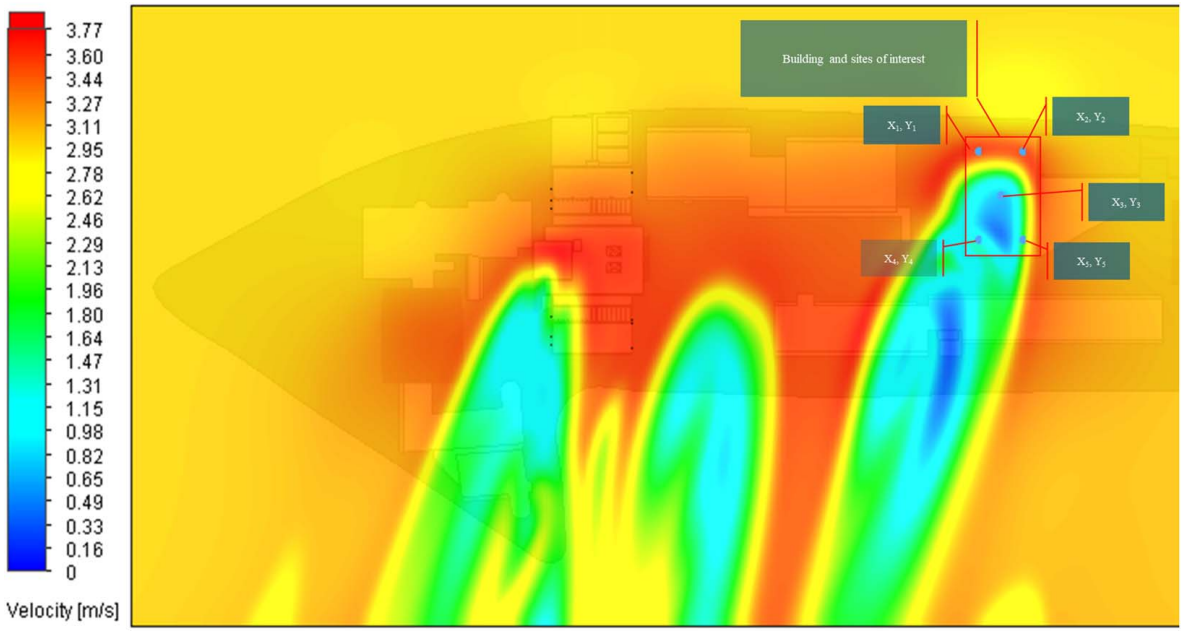

Fig. 6 CFD simulation velocity contour at 34 m elevation, 3 m/s freestream flow

Table 5 Wind speed information from anemometers versus CFD results at positions of interest

Freestream velocity (m/s)	Occurrence (h)	Wind speed at positions of interest from modeling results (m/s)				
		X_1, Y_1	X_2, Y_2	X_3, Y_3	X_4, Y_4	X_5, Y_5
1	1380	1.1	1.1	0.1	0.3	0.1
2	2142	2.3	2.3	0.4	1.1	0.9
3	2106	3.5	3.5	0.6	1.8	1.2
4	1554	4.7	4.6	0.8	2.5	1.6
5	908	5.9	5.8	0.9	3.3	1.9
6	430	7.1	6.9	1.1	4.0	2.4
7	167	8.3	8.1	1.3	4.7	2.8
8	72	9.5	9.3	1.5	5.5	3.2

Table 6 Power generation based on anemometers records and CFD results at positions of interest

Free flow speed (m/s)	Power at anemometer position and x, y position (W)					
	At anemometer	X_1, Y_1	X_2, Y_2	X_3, Y_3	X_4, Y_4	X_5, Y_5
2	10	16	0	0	0	0
3	34	56	0	0	0	0
4	83	136	130	0	20	0
5	165	271	257	0	44	0
6	289	481	453	0	83	17
7	465	776	729	0	140	28
8	701	1175	1101	0	220	43

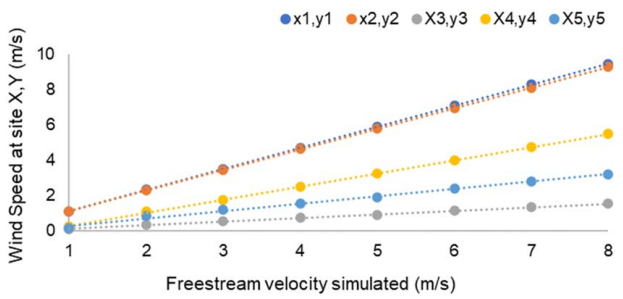

Fig. 7 Wind speed at site versus freestream velocity simulated

plane tool was utilized to increase the cell density in the areas of interest, further enhancing the accuracy of the simulations. This comprehensive approach to meshing and refinement ensures that the CFD simulations capture the intricacies of the wind flow and provide reliable results for analysis. A mesh independent test was conducted to ensure accurate and reliable results. This test involved varying the mesh size and analyzing the impact on the solution. By comparing the results obtained with different mesh sizes, the optimal mesh size that provides consistent results was determined. This process eliminates any potential errors or inconsistencies caused by an inadequate mesh, enhancing the overall accuracy of the simulation. A summary of the mesh test for the case is shown in Table 3, where it can be observed the relative error stabilization of about 9.8% with the mesh refinement.

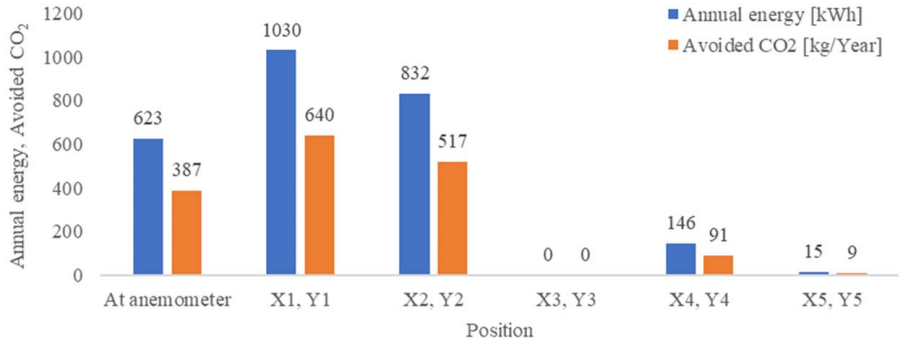

Fig. 8 Annual energy generation and Avoided CO_2 emissions at site characterized by the anemometers and by CFD simulations

For validation purposes, a series of modeling exercises were conducted. These exercises involved defining the parameters of the freestream and configuring the software settings. Subsequently, the software was run, and the results obtained from the modeling were compared with the measured parameters at a specific point. In this case, the freestream velocity and direction were determined based on the data reported in the NASA database at a height of 50 m for the INTEC location. These datasets were collected for the date specified in Table 4. The wind parameters measured during the same period were also recorded and are presented in Table 4. After conducting the modeling exercises, the measured datasets were compared with the modeling results, and the relative error was calculated. Table 4 provides a summary of the validation results. The average error is 3.5%, below 5% is considered acceptable.

Figure 6 depicts a top view of the velocity contour at 3 m/s and 15 deg, obtained through CFD simulations. The results illustrate the distribution of wind across the campus and the presence of high-speed zones around buildings. Additionally, are highlighted potential locations for the installation of SWTs on the EL building. It is important to note the significant variations in wind speed observed across different sites of interest. This observation emphasizes how the energy generation of a SWT can vary considerably depending on the specific installation site, even when located on the same roof.

Table 5 provides a summary of the analysis conducted on wind speed behavior, comparing measurements obtained from anemometers near the studied building with the wind behavior analyzed through CFD analysis. Figure 7 illustrates the differences in wind speed observed for the different positions on the roof, it should be noted that even when the horizontal positions are not significantly different (below 10 m) at higher freestream velocity the differences in wind speed at positions increase.

According to the wind characteristics, a Darrieus-Type H-rotor VAWT was chosen due to the high performance in low wind speed regimes. The SWT's characteristics are 2.4 kW at a wind speed of 12.5 m/s, and 5 m^2 of swept area is presented [16]. The power curve was estimated using the Least Squares Method. The best fit is presented in Eq. (16), with a correlation coefficient of 0.9944. Here, y is the power delivered by SWT in Watts and x is the wind speed in (m/s).

$$y = 1.1501x^{3.0842} \tag{16}$$

Table 6 provides an overview of the estimated annual power generation that can be achieved by a VAWT installed at each sensor position within the specified wind speed.

Figure 8 visually demonstrates the significant variations in energy generation that can occur depending on the specific installation site of a wind turbine, even when located on the same roof. This emphasizes the importance of careful site selection to optimize energy generation. Furthermore, Fig. 8 presents the estimated annual power and energy generation by a VAWT installed at each modeled positions on the roof of interest within the given speed ranges. Notably, the Anem2-INTEC position has the most potential, capable of generating 1030 kWh/year. It should be noted that this energy per turbine is small compared to what the building demands. According to the nine residential consumption profiles presented by Garabitos Lara et al. [90], residential consumption in one ranges between 242 and 1594 kWh/month. These consumptions depend on multiple behavioral factors of residents, such as socioeconomic level, environmental awareness, and other cultural aspects. However, to the extent that the roofs are higher above the ground, higher wind speeds are expected and therefore greater annual energy produced, which may have a better utilization factor from 80 m in height, as well as a more competitive LCOE [45].

Taking into account the estimated AEP and emission factor of 0.62 tCO_2e/MWh, it is projected that placing a SWT in the best location could potentially help avoid emitting 0.640 tCO_{2e} into the atmosphere [81]. This highlights the environmental benefits of selecting the optimal installation site for SWTs.

5 Conclusions

The study focuses on the optimal positioning of SWTs in urban buildings, intending to promote energy sufficiency in urban areas. A robust framework consisting of seven steps was developed: site selection, evaluating urban wind energy using computational fluid dynamics (CFD) simulation and on-site measurements, selecting an appropriate SWT, estimating the annual energy production (AEP), evaluating the environmental impact, resilience, and economic analysis, and finally, installing the system. The paper highlighted the use of CFD simulations in assessing wind energy potential and optimizing the positioning of SWTs on building roofs. Several studies demonstrated the effectiveness of CFD simulations in analyzing wind flow patterns and determining optimal SWTs placement thresholds.

By following this comprehensive framework, it is possible to assess the viability of wind energy utilization in urban areas. A case study was carried out at INTEC university, where on-site measurement campaigns and CFD simulation analysis were used. The average wind speed measured was about 2.49 m/s at 22.5 m height, which is considered low. At 34 m, the average wind speed was estimated to be 3.05 m/s. The predominant wind direction with the greatest intensity was registered at 15 deg respect to the north. The findings of the study showed that the most suitable place for installation had an estimated AEP of around 1030 kWh, which means that only one SWT could lead to a reduction of 640 kg of CO_2 per year.

The study also highlighted the significant impact of the building's geometry on wind flow and energy generation. It was observed how a substantial decrease in wind speed for different positions in the same roof occurs, and its impact on power generation. For instance, for a freestream speed of 4 m/s, a decrease in wind speed from

4.7 m/s to 2.5 m/s was determined in the southwest sensor position (X_4,Y_4) regarding the northeast (X_2,Y_2). With less kinetic energy available, SWTs generate less power, which represents a significant energy drop. This emphasizes the importance of considering wind patterns and selecting optimal sites to maximize energy generation in urban wind energy projects. The findings emphasize the potential of rooftop-mounted turbines in promoting energy sufficiency, reducing emissions, and addressing climate change.

The study also emphasized the significance of energy efficiency in buildings, as they account for a significant share of global energy consumption. SWTs were identified as a potential solution to support the shift towards low-carbon energy and improve urban energy efficiency. The proximity of urban areas to energy demand makes distributed generation technologies like SWTs and solar PV systems particularly suitable.

Acknowledgment

The first author expresses sincere gratitude for the financial support provided by FONDO NACIONAL DE INNOVACIÓN Y DESARROLLO CIENTÍFICO Y TECNOLÓGICO, Grant No. 2022-3C1-141, through the Ministry of Higher Education, Science and Technology (MESCYT) from the Dominican Republic. Additionally, special thanks are extended to Johemil Ramírez for the valuable assistance in proofreading and editing the manuscript.

Conflict of Interest

There are no conflicts of interest.

Data Availability Statement

The datasets generated and supporting the findings of this article are obtainable from the corresponding author upon reasonable request.

Nomenclature

c = scale factor (m/s)
k = shape factor
A = swept area (m^2)
C_p = power coefficient
V_{avg} = average wind speed (m/s)
V_i = desired velocity at height Z_i (m/s)
V_0 = known velocity at height Z_0 (m/s)
Z_i = height 2 (m)
Z_0 = height 1 (m)
$p(V_{avg})$ = Weibull probability density function (%)
α = Hellmann exponent
ρ = air density (kg/m^3)

References

[1] C3S, "Surface Air Temperature for August 2022." https://climate.copernicus.eu/surface-air-temperature-august-2022, Accessed April 13, 2023.
[2] EIA. https://www.eia.gov/tools/faqs/faq.php?id=709&t=6, Accessed February 27, 2024.
[3] Neumeier, M., Cöster, M., Marques Pais, R. A., and Levedag, S., 2022, "State of the Art of Windthermal Turbines: A Systematic Scoping Review of Direct Wind-to-Heat Conversion Technologies," ASME J. Energy Resour. Technol., **144**(4), p. 040802.
[4] Al-Ghussain, L., Ahmad, A. D., Abubaker, A. M., Hovi, K., Hassan, M. A., and Annuk, A., 2023, "Techno-Economic Feasibility of Hybrid PV/Wind/Battery/Thermal Storage Trigeneration System: Toward 100% Energy Independency and Green Hydrogen Production," Energy Rep., **9**, pp. 752–772.
[5] TRADING ECONOMICS, "EU Natural Gas – 2022 Data." https://tradingeconomics.com/commodity/eu-natural-gas, Accessed May 13, 2023.
[6] Ember, "Global Electricity Review 2022." Ember. https://ember-climate.org/insights/research/global-electricity-review-2022/, Accessed September 13, 2022.
[7] Chen, S., Zhang, G., Xia, X., Setunge, S., and Shi, L., 2020, "A Review of Internal and External Influencing Factors on Energy Efficiency Design of Buildings," Energy Build., **216**, p. 109944.
[8] Kim, D., Tran, K., Koh, J., and Cho, H., 2023, "Evaluation of Multi-Functional Variable Refrigerant Flow System With Thermal Energy Storage and Photovoltaic-Based Distributed System for Net-Zero Energy Home Design," ASME J. Energy Resour. Technol., **145**(10), p. 100903.
[9] Millward-Hopkins, J. T., Tomlin, A. S., Ma, L., Ingham, D. B., and Pourkashanian, M., 2013, "Assessing the Potential of Urban Wind Energy in a Major UK City Using an Analytical Model," Renewable Energy, **60**, pp. 701–710.
[10] Karthikeya, B. R., Negi, P. S., and Srikanth, N., 2016, "Wind Resource Assessment for Urban Renewable Energy Application in Singapore," Renewable Energy, **87**, pp. 403–414.
[11] Al-Quraan, A., Stathopoulos, T., and Pillay, P., 2016, "Comparison of Wind Tunnel and On Site Measurements for Urban Wind Energy Estimation of Potential Yield," J. Wind Eng. Ind. Aerodyn., **158**, pp. 1–10.
[12] Wang, Q., Wang, J., Hou, Y., Yuan, R., Luo, K., and Fan, J., 2018, "Micrositing of Roof Mounting Wind Turbine in Urban Environment: CFD Simulations and Lidar Measurements," Renewable Energy, **115**, pp. 1118–1133.
[13] Yang, A.-S., Su, Y.-M., Wen, C.-Y., Juan, Y.-H., Wang, W.-S., and Cheng, C.-H., 2016, "Estimation of Wind Power Generation in Dense Urban Area," Appl. Energy, **171**, pp. 213–230.
[14] Simões, T., and Estanqueiro, A., 2016, "A New Methodology for Urban Wind Resource Assessment," Renewable Energy, **89**, pp. 598–605.
[15] Toja-Silva, F., Colmenar-Santos, A., and Castro-Gil, M., 2013, "Urban Wind Energy Exploitation Systems: Behaviour Under Multidirectional Flow Conditions – Opportunities and Challenges," Renewable Sustainable Energy Rev., **24**, pp. 364–378.
[16] Rezaeiha, A., Montazeri, H., and Blocken, B., 2020, "A Framework for Preliminary Large-Scale Urban Wind Energy Potential Assessment: Roof-Mounted Wind Turbines," Energy Convers. Manage., **214**, p. 112770.
[17] Tasneem, Z., Al Noman, A., Das, S. K., Saha, D. K., Islam, M. R., Ali, M. F., Badal, M. F., Ahamed, M. H., Moyeen, S. I., and Alam, F., 2020, "An Analytical Review on the Evaluation of Wind Resource and Wind Turbine for Urban Application: Prospect and Challenges," Dev. Built Environ., **4**, pp. 100033.
[18] Fields, J., Oteri, F., Preus, R., and Baring-Gould, I., 2016,"Deployment of Wind Turbines in the Built Environment: Risks, Lessons, and Recommended Practices," Report No. NREL/TP–5000-65622, 1260340.
[19] Gagliano, A., Nocera, F., Patania, F., and Capizzi, A., 2013, "Assessment of Micro-Wind Turbines Performance in the Urban Environments: an Aided Methodology Through Geographical Information Systems," Int. J. Energy Environ. Eng., **4**(1), p. 43.
[20] Dhunny, A. Z., Lollchund, M. R., and Rughooputh, S. D. D. V., 2017, "Wind Energy Evaluation for a Highly Complex Terrain Using Computational Fluid Dynamics (CFD)," Renewable Energy, **101**, pp. 1–9.
[21] Toparlar, Y., Blocken, B., Maiheu, B., and van Heijst, G. J. F., 2017, "A Review on the CFD Analysis of Urban Microclimate," Renewable Sustainable Energy Rev., **80**, pp. 1613–1640.
[22] Stathopoulos, T., Alrawashdeh, H., Al-Quraan, A., Blocken, B., Dilimulati, A., Paraschivoiu, M., and Pilay, P., 2018, "Urban Wind Energy: Some Views on Potential and Challenges," J. Wind Eng. Ind. Aerodyn., **179**, pp. 146–157.
[23] Toja-Silva, F., Kono, T., Peralta, C., Lopez-Garcia, O., and Chen, J., 2018, "A Review of Computational Fluid Dynamics (CFD) Simulations of the Wind Flow Around Buildings for Urban Wind Energy Exploitation," J. Wind Eng. Ind. Aerodyn., **180**, pp. 66–87.
[24] Arteaga-López, E., Ángeles-Camacho, C., and Bañuelos-Ruedas, F., 2019, "Advanced Methodology for Feasibility Studies on Building-Mounted Wind Turbines Installation in Urban Environment: Applying CFD Analysis," Energy, **167**, pp. 181–188.
[25] Juan, Y.-H., Wen, C.-Y., Li, Z., and Yang, A.-S., 2021, "Impacts of Urban Morphology on Improving Urban Wind Energy Potential for Generic High-Rise Building Arrays," Appl. Energy, **299**, p. 117304.
[26] Ricci, A., Burlando, M., Repetto, M. P., and Blocken, B., 2022, "Static Downscaling of Mesoscale Wind Conditions Into an Urban Canopy Layer by a CFD Microscale Model," Build. Environ., **225**, p. 109626.
[27] Padmanabhan, K. K., 2013, "Study on Increasing Wind Power in Buildings Using TRIZ Tool in Urban Areas," Energy Build., **61**, pp. 344–348.
[28] Park, J., Jung, H.-J., Lee, S.-W., and Park, J., 2015, "A New Building-Integrated Wind Turbine System Utilizing the Building," Energies, **8**(10), pp. 11846–11870.
[29] Toja-Silva, F., Lopez-Garcia, O., Peralta, C., Navarro, J., and Cruz, I., 2016, "An Empirical–Heuristic Optimization of the Building-Roof Geometry for Urban Wind Energy Exploitation on High-Rise Buildings," Appl. Energy, **164**, pp. 769–794.
[30] Khoshdel Nikkho, S., Heidarinejad, M., Liu, J., and Srebric, J., 2017, "Quantifying the Impact of Urban Wind Sheltering on the Building Energy Consumption," Appl. Therm. Eng., **116**, pp. 850–865.
[31] Wang, J.-W., Yang, H.-J., and Kim, J.-J., 2020, "Wind Speed Estimation in Urban Areas Based on the Relationships Between Background Wind Speeds and Morphological Parameters," J. Wind Eng. Ind. Aerodyn., **205**, p. 104324.
[32] Vita, G., Shu, Z., Jesson, M., Quinn, A., Hemida, H., Sterling, M., and Baker, C., 2020, "On the Assessment of Pedestrian Distress in Urban Winds," J. Wind Eng. Ind. Aerodyn., **203**, p. 104200.
[33] Arteaga-López, E., and Angeles-Camacho, C., 2021, "Innovative Virtual Computational Domain Based on Wind Rose Diagrams for Micrositing Small Wind Turbines," Energy, **220**, p. 119701.
[34] Juan, Y.-H., Wen, C.-Y., Chen, W.-Y., and Yang, A.-S., 2021, "Numerical Assessments of Wind Power Potential and Installation Arrangements in Realistic Highly Urbanized Areas," Renewable Sustainable Energy Rev., **135**, p. 110165.
[35] Mitkov, R., Pantusheva, M., Naserentin, V., Hristov, P. O., Wästberg, D., Hunger, F., Mark, A., Petrova-Antonova, D., Edelvik, F., and Logg, A., 2022, "Using the

Octree Immersed Boundary Method for Urban Wind CFD Simulations," IFAC-Pap., **55**(11), pp. 179–184.
[36] AL-Yahyai, S., Charabi, Y., Gastli, A., and Al-Alawi, S., 2010, "Assessment of Wind Energy Potential Locations in Oman Using Data From Existing Weather Stations," Renewable Sustainable Energy Rev., **14**(5), pp. 1428–1436.
[37] Gil-García, I. C., García-Cascales, M. S., and Molina-García, A., 2022, "Urban Wind: An Alternative for Sustainable Cities," Energies, **15**(13), p. 4759.
[38] Vallejo-Díaz, A., Herrera-Moya, I., Fernández-Bonilla, A., and Pereyra-Mariñez, C., 2022, "Wind Energy Potential Assessment of Selected Locations at Two Major Cities in the Dominican Republic, Toward Energy Matrix Decarbonization, With Resilience Approach," Therm. Sci. Eng. Prog., **32**, p. 101313.
[39] Vallejo Díaz, A., Herrera Moya, I., Pereyra Mariñez, C., Garabitos Lara, E., and Casilla Victorino, C., 2023, "Key Factors Influencing Urban Wind Energy: A Case Study From the Dominican Republic," Energy Sustainable Dev., **73**, pp. 165–173.
[40] Suhanda, R. D. P., and Pratami, D., 2021, "RACI Matrix Design for Managing Stakeholders in Project Case Study of PT. XYZ," Int. J. Innov. Enterp. Syst., **5**(2), pp. 122–133.
[41] Hirmer, S. A., George-Williams, H., Rhys, J., McNicholl, D., and McCulloch, M., 2021, "Stakeholder Decision-Making: Understanding Sierra Leone's Energy Sector," Renewable Sustainable Energy Rev., **145**, p. 111093.
[42] Lee, W., Lee, S., Jin, C., and Hyun, C., 2021, "Development of the RACI Model for Processes of the Closure Phase in Construction Programs," Sustainability, **13**(4), p. 1806.
[43] Vallejo Díaz, A., Herrera Moya, I., Garabitos Lara, E., and Casilla Victorino, C. K., 2024, "Assessment of Urban Wind Potential and the Stakeholders Involved in Energy Decision-Making," Sustainability, **16**(4), pp. 1362.
[44] Kiunke, T., Gemignani, N., Malheiro, P., and Brudermann, T., 2022, "Key Factors Influencing Onshore Wind Energy Development: A Case Study From the German North Sea Region," Energy Policy, **165**, p. 112962.
[45] Vallejo, A., Herrera, I., Malmquist, A., Elmegaard, B., Sciubba, E., MBlanco-Marigorta, A., Jensen, J. K., et al., 2022, "Building-Mounted Wind Energy Potential in Santo Domingo, the Dominican Republic, a Contribution for Resilient Decarbonisation," Proceedings of ECOS 2022 – The 35th International Conference on Efficiency, Cost, Optimization, Simulation and Environmental Impact of Energy Systems, Copenhagen, Denmark, July 3–7, B. Elmegaard, E. Sciubba, A. MBlanco-Marigorta, J. K. Jensen, W. B. Markussen, W. Meesenburg, N. A. Kermani, T. Zhu, and R. Kofler, eds., Danmarks Tekniske Universitet (DTU), Lyngby Denmark, pp. 1925–1936.
[46] Xu, Y., Li, Y., Zheng, L., Cui, L., Li, S., Li, W., and Cai, Y., 2020, "Site Selection of Wind Farms Using GIS and Multi-Criteria Decision Making Method in Wafangdian, China," Energy, **207**, p. 118222.
[47] Mittal, H., Sharma, A., and Gairola, A., 2018, "A Review on the Study of Urban Wind at the Pedestrian Level Around Buildings," J. Build. Eng., **18**, pp. 154–163.
[48] Du, S., Zhang, X., Jin, X., Zhou, X., and Shi, X., 2022, "A Review of Multi-Scale Modelling, Assessment, and Improvement Methods of the Urban Thermal and Wind Environment," Build. Environ., **213**, p. 108860.
[49] Garuma, G. F., 2018, "Review of Urban Surface Parameterizations for Numerical Climate Models," Urban Clim., **24**, pp. 830–851.
[50] Peng, H. Y., Dai, S. F., Lin, K., Hu, G., and Liu, H. J., 2020, "Experimental Investigation of Wind Characteristics and Wind Energy Potential Over Rooftops: Effects of Building Parameters," J. Wind Eng. Ind. Aerodyn., **205**, p. 104304.
[51] Oke, T. R., 2002, *Boundary Layer Climates*, Routledge, London, UK.
[52] Škvorc, P., and Kozmar, H., 2021, "Wind Energy Harnessing on Tall Buildings in Urban Environments," Renewable Sustainable Energy Rev., **152**, p. 111662.
[53] Islam, M. R., Saidur, R., and Rahim, N. A., 2011, "Assessment of Wind Energy Potentiality at Kudat and Labuan, Malaysia Using Weibull Distribution Function," Energy, **36**(2), pp. 985–992.
[54] Gualtieri, G., and Secci, S., 2011, "Wind Shear Coefficients, Roughness Length and Energy Yield Over Coastal Locations in Southern Italy," Renewable Energy, **36**(3), pp. 1081–1094.
[55] Anderson, M., and Beyene, A., 2015, "Integrated Resource Mapping of Wave and Wind Energy," ASME J. Energy Resour. Technol., **138**, p. 011203.
[56] Kc, A., Whale, J., and Urmee, T., 2019, "Urban Wind Conditions and Small Wind Turbines in the Built Environment: A Review," Renewable Energy, **131**, pp. 268–283.
[57] Emejeamara, F. C., and Tomlin, A. S., 2020, "A Method for Estimating the Potential Power Available to Building Mounted Wind Turbines Within Turbulent Urban air Flows," Renewable Energy, **153**, pp. 787–800.
[58] NASA, "Implementing Turbulence Models into the Compressible RANS Equations." https://turbmodels.larc.nasa.gov/implementrans.html, Accessed April 3, 2023.
[59] SOLIDWORKS, "Numerical Basis of CAD-Embedded CFD." https://www.solidworks.com/sw/docs/flow_basis_of_cad_embedded_cfd_whitepaper.pdf, Accessed April 3, 2023.
[60] Van Treuren, K. W., and Hays, A. W., 2017, "A Study of Noise Generation on the E387, S823, NACA 0012, and NACA 4412 Airfoils for Use on Small-Scale Wind Turbines in the Urban Environment," ASME J. Energy Resour. Technol., **139**(5), p. 051217.
[61] SOLIDWORKS, "SOLIDWORKS Flow Simulation." SOLIDWORKS. https://www.solidworks.com/es/product/solidworks-flow-simulation, Accessed April 3, 2023.
[62] Ighodaro, O., and Akhihiero, D., 2021, "Modeling and Performance Analysis of a Small Horizontal Axis Wind Turbine," ASME J. Energy Resour. Technol., **143**(3), p. 031301.
[63] Zagubień, A., and Wolniewicz, K., 2022, "Energy Efficiency of Small Wind Turbines in an Urbanized Area – Case Studies," Energies, **15**(14), p. 5287.
[64] Siram, O., Kumar, R., Saha, U. K., and Sahoo, N., 2022, "Wind Tunnel Probe Into an Array of Small-Scale Horizontal-Axis Wind Turbines Operating at Low Tip Speed Ratio Conditions," ASME J. Energy Resour. Technol., **144**(9), p. 091303.
[65] Micallef, D., and Van Bussel, G., 2018, "A Review of Urban Wind Energy Research: Aerodynamics and Other Challenges," Energies, **11**(9), p. 2204.
[66] Amano, R. S., 2017, "Review of Wind Turbine Research in 21st Century," ASME J. Energy Resour. Technol., **139**(5), p. 050801.
[67] Naik, K., and Sahoo, N., 2023, "Synergistic Effect of J-Shape Airfoil on the Performance of Darrieus-Type Straight-Bladed Vertical Axis Wind Turbine," ASME J. Energy Resour. Technol., **145**(10), p. 101301.
[68] IEC 61400-2:2013, 2013. https://webstore.iec.ch/publication/5433
[69] Ismail, K. A. R., Canale, T., and Lino, F. A. M., 2022, "Effects of the Airfoil Section, Chord and Twist Angle Distributions on the Starting Torque of Small Horizontal Axis Wind Turbines," ASME J. Energy Resour. Technol., **144**(5), p. 051301.
[70] Eriksson, S., Bernhoff, H., and Leijon, M., 2008, "Evaluation of Different Turbine Concepts for Wind Power," Renewable Sustainable Energy Rev., **12**(5), pp. 1419–1434.
[71] Tummala, A., Velamati, R. K., Sinha, D. K., Indraja, V., and Krishna, V. H., 2016, "A Review on Small Scale Wind Turbines," Renewable Sustainable Energy Rev., **56**, pp. 1351–1371.
[72] Tan, J. D., Chang, C. C. W., Bhuiyan, M. A. S., Minhad, K. N., and Ali, K., 2022, "Advancements of Wind Energy Conversion Systems for Low-Wind Urban Environments: A Review," Energy Rep., **8**, pp. 3406–3414.
[73] Lipian, M., Dobrev, I., Massouh, F., and Jozwik, K., 2020, "Small Wind Turbine Augmentation: Numerical Investigations of Shrouded- and Twin-Rotor Wind Turbines," Energy, **201**, p. 117588.
[74] Ghoneam, S. M., Hamada, A. A., and Sherif, T. S., 2024, "Fatigue-Life Estimation of Vertical-Axis Wind Turbine Composite Blades Using Modal Analysis," ASME J. Energy Resour. Technol., **146**(3), p. 031301.
[75] Abohela, I., Hamza, N., and Dudek, S., 2013, "Effect of Roof Shape, Wind Direction, Building Height and Urban Configuration on the Energy Yield and Positioning of Roof Mounted Wind Turbines," Renewable Energy, **50**, pp. 1106–1118.
[76] DOE, "Distributed Wind Market Report: 2022 Edition." Energy.gov. https://www.energy.gov/eere/wind/articles/distributed-wind-market-report-2022-edition, Accessed March 10, 2023.
[77] Sharma, K., and Ahmed, M. R., 2016, "Wind Energy Resource Assessment for the Fiji Islands: Kadavu Island and Suva Peninsula," Renewable Energy, **89**, pp. 168–180.
[78] Olatayo, K. I., Wichers, J. H., and Stoker, P. W., 2018, "Energy and Economic Performance of Small Wind Energy Systems Under Different Climatic Conditions of South Africa," Renewable Sustainable Energy Rev., **98**, pp. 376–392.
[79] Dastjerdi, B., Strezov, V., Kumar, R., and Behnia, M., 2022, "Environmental Impact Assessment of Solid Waste to Energy Technologies and Their Perspectives in Australia," Sustainability, **14**(23), p. 23.
[80] Guerrero-Liquet, G. C., Sánchez-Lozano, J. M., García-Cascales, M. S., Lamata, M. T., and Verdegay, J. L., 2016, "Decision-Making for Risk Management in Sustainable Renewable Energy Facilities: A Case Study in the Dominican Republic," Sustainability, **8**(5), p. 455.
[81] Chen, H., Yao, S., Peng, K., Zhou, S., and Tian, P., 2023, "Grid Emission Factors: The Key to Greenhouse Gas Emission Accounting," Resour. Conserv. Recycl., **190**, p. 106846.
[82] UNFCCC, "Grid Emission Factor for the Dominican Republic (Version 01.0)." https://cdm.unfccc.int/methodologies/standard_base/2015/sb143.html, Accessed May 15, 2021.
[83] Umunnakwe, A., Huang, H., Oikonomou, K., and Davis, K. R., 2021, "Quantitative Analysis of Power Systems Resilience: Standardization, Categorizations, and Challenges," Renewable Sustainable Energy Rev., **149**, p. 111252.
[84] Selga, A. G., Muñoz, D. S., and Dominguez-García, J. L., 2022, "Analysis and Enhancement of Barcelona's Power Grid Resilience," Energy Rep., **8**, pp. 1160–1167.
[85] Wang, Y., Yang, Y., and Xu, Q., 2023, "Resilience Assessment of the Integrated Gas and Power Systems Under Extreme Weather," Energy Rep., **9**, pp. 160–167.
[86] WMO, "Tropical Cyclones." https://public.wmo.int/en/our-mandate/focus-areas/natural-hazards-and-disaster-risk-reduction/tropical-cyclones, Accessed September 10, 2022.
[87] Sunderland, K. M., Narayana, M., Putrus, G., Conlon, M. F., and McDonald, S., 2016, "The Cost of Energy Associated With Micro Wind Generation: International Case Studies of Rural and Urban Installations," Energy, **109**, pp. 818–829.
[88] Aldersey-Williams, J., and Rubert, T., 2019, "Levelised Cost of Energy – A Theoretical Justification and Critical Assessment," Energy Policy, **124**, pp. 169–179.
[89] W. M. Organization (WMO), "Guide to Instruments and Methods of Observation." https://library.wmo.int/records/item/68660-guide-to-instruments-and-methods-of-observation, Accessed February 27, 2024.
[90] Garabitos Lara, E., Vallejo Díaz, A., Ocaña Guevara, V. S., and Santos García, F., 2023, "Techno-Economic Evaluation of Residential PV Systems Under a Tiered Rate and Net Metering Program in the Dominican Republic," Energy Sustainable Dev., **72**, pp. 42–57.